Formal Analysis of Networked Microgrids Dynamics

Yan Li, *Student Member, IEEE*, Peng Zhang, *Senior Member, IEEE*, and Peter B. Luh, *Life Fellow, IEEE*

***Abstract*—A formal analysis via reachable set computation (FAR) is presented to efficiently assess the stability of networked microgrids in the presence of heterogeneous uncertainties induced by high penetration of distributed energy resources. FAR with mathematical rigor directly computes the bounds of all possible dynamic trajectories and provides stability information unattainable by traditional time-domain simulations or direct methods. An advanced Geršgorin theory with a quasi-diagonalization technique is then combined with FAR to estimate eigenvalues of those scenarios pertaining to the reachable set boundary to identify systems' stability margins. Extensive tests show that FAR enables efficient analysis on impacts of disturbances on networked microgrid dynamics and offers a potent tool to evaluate how far the networked microgrid system is from its stability margins. These salient features make FAR a powerful tool for planning, designing, monitoring, and operating future networked microgrids.**

***Index Terms*—Networked microgrids, stability, formal analysis, reachable set, uncertainties, Geršgorin theory, eigen-analysis, power-electronics interface, distributed energy resources (DERs).**

I. Introduction

MICROGRID is an emerging and promising paradigm to enhance electricity resiliency for customers [1]. It is a potent option to alleviate and prevent power outages locally because of its capability of autonomous operations, flexibility in accommodating distributed energy resources (DERs), and immunity to stormy weather damages. However, a single microgrid can hardly contribute to the resiliency of main distribution grids [2], despite the significant resiliency benefit to local customers. Coordinative networked microgrids, i.e., a cluster of microgrids interconnected in close electrical or spatial proximity with coordinated energy management and interactive supports and exchanges [3], [4], can potentially help restore neighboring distribution grids after a major blackout. They can significantly improve day-to-day reliability performance, meanwhile impacting the stability of grids.

The low inertia nature of power-electronics interfaces of DERs makes microgrids highly sensitive to disturbances; and thus, deteriorates the stability of microgrids, even though these interfaces enables high penetration of DERs and flexible dispatch and control [5]. These disturbances could be uncontrollable external events (e.g., grid faults), variation in system structure and parameters (e.g., creation of sub-microgrids), or disturbances from generation side or consumption (e.g., PV, wind, electric vehicles), etc. The challenge here is that the above stability issue could rapidly escalate when microgrids are interconnected. Understanding and quantifying the transient stability feature of power-electronics-dominated networked microgrids under virtually infinite number of scenarios is an intractable problem.

There exist two major categories of dynamic assessment methods, time domain simulation and direct methods [6], [7], which could also be applicable to networked microgrids. In time domain simulation, trajectories of state variables are computed based on specified system structure and initial conditions [8]. This approach is known to be inefficient in handling parametric or input uncertainties. Although Monte Carlo runs could be adopted, it is still difficult to verify the infinitely many scenarios that can happen in a real system [9]. Direct methods can compute regions of attraction which is unattainable with time domain simulation methods, and can be used to quickly check if control actions are capable of stabilizing systems. The limitations of direct methods in assessing networked microgrids performance include: (1) the difficulty in constructing an appropriate Lyapunov function [10] or contraction function [11], (2) significant reduction of system models resulting in inexact prediction [12], [13], and (3) ineffectiveness in dealing with ubiquitous uncertainties [14], [15]. Besides, numerical solvers for direct methods, e.g., sum of squares and semi-definite programming [16], are still too complex to be scalable for networked microgrids.

In order to overcome the limitations of existing methods, a formal analysis via reachable set computation (FAR) is presented in this paper. Specifically, small signal stability under different disturbances is analyzed to efficiently assess the stability of networked microgrids. FAR is further combined with a quasi-diagonalization-based Geršgorin theory to efficiently probe the boundary of the stability region subject to uncertainties [17]–[19]. The novelties of the FAR method are threefold:

1) It is an on-the-fly solution that directly obtains possible operation ranges for networked microgrids subject to disturbances.
2) FAR provides reachable set information that pinpoints critical disturbances and is useful for predictive control and dispatch to enhance networked microgrid stability.
3) The reachable set results can be used to accurately estimate the stability margin of networked microgrids under uncertainties.

Manuscript received August 1, 2017; revised October 31, 2017; accepted November 30, 2017. Date of publication December 6, 2017; date of current version April 17, 2018. This work was supported by the National Science Foundation under Award nos. CNS-1647209 and EECS-1611095. Paper no. TPWRS-01177-2017. *(Corresponding author: Peng Zhang.)*

The authors are with the Department of Electrical and Computer Engineering, University of Connecticut, Storrs, CT 06269 USA (e-mail: yan.7.li@uconn.edu; peng.zhang@uconn.edu; Peter.Luh@uconn.edu).

Color versions of one or more of the figures in this paper are available online at http://ieeexplore.ieee.org.

Digital Object Identifier 10.1109/TPWRS.2017.2780804

These salient features make FAR a powerful tool beyond direct methods and time domain simulations while incorporating the benefits of both.

The remainder of this paper is organized as follows: Section II establishes the methodological foundations of FAR, and Section III describes quasi-diagonalization-based Geršgorin theorem and its integration with FAR. Section IV analyzes impacts of disturbances in networked microgrids. Section V presents the implementation of FAR with Geršgorin. In Section VI, tests on networked microgrids verify the feasibility and effectiveness of the presented approach. Conclusions are drawn in Section VII.

II. Formal Analysis Via Reachable Set

FAR aims at finding the bounds of all possible system trajectories under various disturbances. Mathematically, the aim is to find a reachable set, where one viable solution can be presented as follows: first, the original nonlinear differential-algebraic equations (DAEs) of a dynamic system are abstracted into linear differential inclusions at each time step, obtaining a finite-dimensional state matrix of the system $\mathbf{A} = [a_{ij}] \in \mathbb{R}^{n\times n}$. Its reachability analysis under uncertainties can then be expressed as follows:

$$\Delta\dot{\mathbf{x}} \in \mathbf{A}\Delta\mathbf{x} \oplus \mathbf{P}, \tag{1}$$

where $\Delta\mathbf{x} = \mathbf{x} - \mathbf{x_0}$, $\mathbf{x_0}$ is the operation point where the system is linearized, $\mathbf{P}$ is a set of uncertain inputs which can be formulated using a set-based approach, and $\oplus$ is Minkowski addition.

Second, a reachable set can be obtained at each simulation time step via a closed-form solution [17], [18]:

$$\mathcal{R}^e(t_{k+1}) = \phi(\mathbf{A}, r)\mathcal{R}^e(t_k) \oplus \Psi(\mathbf{A}, r, \mathbf{p_0}) \oplus I_p^e(\mathbf{p_\Delta}, r), \tag{2}$$

$$\begin{aligned}\mathcal{R}^e(\tau_k) = {} & C(\mathcal{R}^e(t_k), \phi(\mathbf{A}, r)\mathcal{R}^e(t_k) \oplus \Psi(\mathbf{A}, r, \mathbf{p_0})) \\ & \oplus I_p^e(\mathbf{p_\Delta}, r) \oplus I_\xi^e,\end{aligned} \tag{3}$$

where $\mathcal{R}^e(t_{k+1})$ is the reachable set at each time step, $\mathcal{R}^e(\tau_k)$ is the reachable set during time steps, $\phi(\mathbf{A}, r)$ represents how the history reachable set $\mathcal{R}^e(t_k)$ contributes to the current one, as expressed in (4), $\Psi(\mathbf{A}, r, \mathbf{p_0})$ and $I_p^e(\mathbf{p_\Delta}, r)$ represent the increment of reachable set caused by deterministic inputs $\mathbf{p_0}$ and uncertain ones $\mathbf{p_\Delta}$, as expressed in (5) and (6), respectively, I_ξ^e represents increment in reachable set caused by curvature of trajectories from t_k to t_{k+1}, as shown in (7), $r = t_{k+1} - t_k$ is the time interval, and $C(\cdot)$ represents convex hull calculation [17].

$$\phi(\mathbf{A}, r) = e^{\mathbf{A}r}, \tag{4}$$

$$\Psi(\mathbf{A}, r, \mathbf{p_0}) = \left\{ \sum_{i=0}^{\eta} \frac{\mathbf{A}^i r^{i+1}}{(i+1)!} \oplus \big[-X(\mathbf{A}, r)r, X(\mathbf{A}, r)r\big] \right\}\mathbf{p_0}, \tag{5}$$

$$\begin{aligned}I_p^e(\mathbf{p_\Delta}, r) = {} & \sum_{i=0}^{\eta} \left(\frac{\mathbf{A}^i r^{i+1}}{(i+1)!}\mathbf{p_\Delta} \right) \\ & \oplus \left\{ \big[-X(\mathbf{A}, r)r, X(\mathbf{A}, r)r\big] \cdot \mathbf{p_\Delta} \right\},\end{aligned} \tag{6}$$

$$\begin{aligned}I_\xi^e = {} & \left\{ \big(I \oplus [-X(\mathbf{A}, r), X(\mathbf{A}, r)]\big) \cdot \mathcal{R}^e(t_k) \right\} \\ & \oplus \left\{ \big(\tilde{I} \oplus [-X(\mathbf{A}, r)r, X(\mathbf{A}, r)r]\big) \cdot \mathbf{p_0} \right\}.\end{aligned} \tag{7}$$

In (4), $e^{\mathbf{A}r}$ is calculated by integrating the finite Taylor series $\sum_{i=0}^{\eta} \frac{(\mathbf{A}r)^i}{i!}$ up to order η [17]. And $X(\mathbf{A}, r)$, I, $\tilde{I}$ involved in (5)–(7) are given as follows:

$$X(\mathbf{A}, r) = e^{|\mathbf{A}|r} - \sum_{i=0}^{\eta} \frac{(|\mathbf{A}|r)^i}{i!}, \tag{8}$$

$$I = \sum_{i=2}^{\eta} \big[(i^{\frac{-i}{i-1}} - i^{\frac{-1}{i-1}})r^i, 0\big] \frac{\mathbf{A}^i}{i!}, \tag{9}$$

$$\tilde{I} = \sum_{i=2}^{\eta+1} \big[(i^{\frac{-i}{i-1}} - i^{\frac{-1}{i-1}})r^i, 0\big] \frac{\mathbf{A}^{i-1}}{i!}. \tag{10}$$

If necessary, the over-approximation of the reachable set along the time interval can be minimized using advanced techniques such as reachable set splitting or optimality-based bounds tightening, as detailed in [20], [21].

III. Quasi-Diagonalized Geršgorin Theory

In this section, we devise an enhanced Geršgorin theory for estimating the eigenvalues of a dynamical system under disturbances, which will be used for the stability margin estimation in Section V.

The eigenvalue problem at each time step, which reflects the small signal stability feature of a dynamical system, can be described as follows [19].

$$\begin{cases} \mathbf{A}\mathbf{v}_i &= \lambda_i \mathbf{v}_i \\ \mathbf{A}^{\mathrm{T}}\mathbf{u}_i &= \lambda_i \mathbf{u}_i \end{cases} \tag{11}$$

where λ_i is the ith generalized eigenvalue of the system;$\mathbf{v}_i$ and $\mathbf{u}_i^{\mathrm{T}}$ are the ith right and left eigenvector, respectively, satisfying the orthogonal normalization conditions as shown in (12).

$$\begin{cases} \mathbf{u}_i^{\mathrm{T}}\mathbf{v}_j &= \delta_{ij} \\ \mathbf{u}_i^{\mathrm{T}}\mathbf{A}\mathbf{v}_j &= \delta_{ij}\lambda_i \end{cases} \tag{12}$$

where δ_{ij} is the Kronecker sign.

Instead of calculating the exact eigenvalues, based on the state matrix $\mathbf{A}$, the eigenvalue range can be estimated using the Geršgorin disk and set via the following Geršgorin theorem [22], [23]. The reason is that the calculation of exact eigenvalues is tedious, time-consuming, and not always necessary especially when a system is far away from its stability margin.

Theorem 1: For any nonsingular finite-dimensional matrix $\mathbf{A}$ with λ_i as its ith eigenvalue, there is a positive integer k in

N=1,2,...,n such that,

$$|\lambda_i - a_{kk}| \le r_k(\mathbf{A}), \tag{13}$$

where $r_k(\mathbf{A}) \doteq \sum_{j\in N\backslash\{k\}} |a_{kj}|$. If $\sigma(\mathbf{A})$ denotes a set of all eigenvalues of $\mathbf{A}$, then $\sigma(\mathbf{A})$ satisfies the following condition

$$\sigma(\mathbf{A}) \subseteq \Gamma(\mathbf{A}) \doteq \cup_{k=1}^{n} \Gamma_k(\mathbf{A}), \tag{14}$$

where $\Gamma(\mathbf{A})$ is the Geršgorin set of nonsingular matrix $\mathbf{A}$, $\Gamma_k(\mathbf{A})$ is the kth Geršgorin disk, and can be expressed as $\Gamma_k(\mathbf{A}) \doteq \{|x - a_{kk}| \le r_k(\mathbf{A}), x \in \mathbb{R}\}$.

When the state matrix is not strongly diagonally dominant, the estimation of eigenvalue distribution is usually over-approximated. Therefore, a quasi-diagonalized Geršgorin is established as follows to reduce the conservativeness of the conventional Geršgorin theory and to improve the estimation accuracy of eigenvalue distributions.

Taking into account the orthogonal normalization conditions shown in (12), the state matrix $\mathbf{A}$ under system disturbances can be quasi-diagonalized as follows:

$$\mathbf{U}_0^{\mathrm{T}}\mathbf{A}\mathbf{V}_0 = \mathbf{U}_0^{\mathrm{T}}\mathbf{A}_0\mathbf{V}_0 + \mathbf{U}_0^{\mathrm{T}}\mathbf{A}_P\mathbf{V}_0 = \mathbf{S}_0 + \mathbf{S}_P, \tag{15}$$

where $\mathbf{A}_0$ is the system state matrix at $(\mathbf{x}_0, \mathbf{y}_0)$; $\mathbf{S}_0$, $\mathbf{U}_0^{\mathrm{T}}$ and $\mathbf{V}_0$ are the corresponding eigenvalue matrix, left eigenvector matrix, and right eigenvector matrix at $(\mathbf{x}_0, \mathbf{y}_0)$, respectively; $\mathbf{A}_P$ is the increment of state matrix under disturbances, which is constructed based on a bounded set of uncertainties and will be analyzed in next subsection; $\mathbf{S}_P$ is the increment of eigenvalue matrix. Thus, the eigenvalue problem of a disturbed system is transformed to the analysis of the matrix $\mathbf{S}_P$, and the following expression can be obtained:

$$\Gamma_k(\mathbf{S}_P) = \{|x - s_{kk}| \le r_k(\mathbf{S}_P), x \in \mathbb{R}\}, \tag{16}$$

$$\sigma_k(\mathbf{S}_P) \subseteq \Gamma(\mathbf{S}_P) \doteq \cup_{k=1}^{n} \Gamma_k(\mathbf{S}_P). \tag{17}$$

Therefore, the distribution of each eigenvalue in a system under uncertainties can be expressed as a Geršgorin disk with $\mathbf{S}_0$ as its center and $\Gamma_k(\mathbf{S}_P)$ as its corresponding area.

IV. FAR in Networked Microgrids

Networked micgrids as a system can be modeled as a set of semi-explicit, index-1, nonlinear DAEs when power-electronic interfaces are modeled using dynamic averaging, as follows

$$\begin{cases} \dot{\mathbf{x}} = \mathbf{F}(\mathbf{x}, \mathbf{y}, \mathbf{p}) \\ \mathbf{0} = \mathbf{G}(\mathbf{x}, \mathbf{y}, \mathbf{p}) \end{cases} \tag{18}$$

where $\mathbf{x} \in \mathbb{R}^n$ is the state variable vector, $\mathbf{y} \in \mathbb{R}^m$ is the algebraic variable vector, $\mathbf{p} \in \mathbb{R}^p$ is the disturbance vector, which will be formulated using a set-based approach. Linearizing the networked microgrids system at the operation point $(\mathbf{x_0}, \mathbf{y_0}, \mathbf{p_0})$ [17], one can obtain the following equations, when the high-order Taylor expansion is neglected.

$$\begin{cases} \dot{\mathbf{x}} = \mathbf{F}(\mathbf{x_0}, \mathbf{y_0}, \mathbf{p_0}) + \frac{\partial \mathbf{F}}{\partial \mathbf{x}}\Delta\mathbf{x} + \frac{\partial \mathbf{F}}{\partial \mathbf{y}}\Delta\mathbf{y} + \frac{\partial \mathbf{F}}{\partial \mathbf{p}}\Delta\mathbf{p} \\ \mathbf{0} = \mathbf{G}(\mathbf{x_0}, \mathbf{y_0}, \mathbf{p_0}) + \frac{\partial \mathbf{G}}{\partial \mathbf{x}}\Delta\mathbf{x} + \frac{\partial \mathbf{G}}{\partial \mathbf{y}}\Delta\mathbf{y} + \frac{\partial \mathbf{G}}{\partial \mathbf{p}}\Delta\mathbf{p} \end{cases} \tag{19}$$

where $\mathbf{F_x} = \partial\mathbf{F}/\partial\mathbf{x}$ is the partial derivative matrix of differential equations with respect to state variables, $\mathbf{F_y} = \partial\mathbf{F}/\partial\mathbf{y}$ is the partial derivative matrix of differential equations with respect to algebraic variables, $\mathbf{F_p} = \partial\mathbf{F}/\partial\mathbf{p}$ is the partial derivative matrix of differential equations with respect to disturbance variables, $\mathbf{G_x} = \partial\mathbf{G}/\partial\mathbf{x}$ is the partial derivative matrix of algebraic equations with respect to state variables, $\mathbf{G_y} = \partial\mathbf{G}/\partial\mathbf{y}$ is the partial derivative matrix of algebraic equations with respect to algebraic variables, $\mathbf{G_p} = \partial\mathbf{G}/\partial\mathbf{p}$ is the partial derivative matrix of algebraic equations with respect to disturbance variables. When $\mathbf{G_y}$ is nonsingular, the following equation can be obtained [17].

$$\Delta\dot{\mathbf{x}} = [\mathbf{F_x} - \mathbf{F_y}\mathbf{G_y}^{-1}\mathbf{G_x}]\Delta\mathbf{x} + [\mathbf{F_p} - \mathbf{F_y}\mathbf{G_y}^{-1}\mathbf{G_p}]\Delta\mathbf{p}. \tag{20}$$

Therefore, with linearization, a state matrix can be obtained at each time step.

$$\mathbf{A}_{NMG} = \mathbf{F_x} - \mathbf{F_y}\mathbf{G_y}^{-1}\mathbf{G_x}, \tag{21}$$

where, $\mathbf{A}_{NMG}$ is equivalent to $\mathbf{A}$ in (1) and 1, $[\mathbf{F_p} - \mathbf{F_y}\mathbf{G_y}^{-1}\mathbf{G_p}]\Delta\mathbf{p}$ is equivalent to $\mathbf{P}$ in (1).

A. Modeling Disturbances in Networked Microgrids

The key to formal analysis is to properly model uncertain inputs. Instead of using the traditional point-based methods, a set-based approach (e.g., with zonotope, ellipsoid, polytopes) is adopted to better quantify these uncertainties [17]. Zonotopes are recommended because they are computationally both efficient and stable, closed under Minkowski operations, and suitable for convex hull computations and convex optimization. Moreover, those 'unknown but bounded' intervals, polytopes, and ellipsoids based uncertainties in networked microgrids can be easily converted to zonotopes.

A zonotope $\mathcal{P}$ is usually parameterized by a center and generators as follows [17], [18]:

$$\mathcal{P} = \left\{ \boldsymbol{c} + \sum_{i=1}^{m} \beta_i \boldsymbol{g}_i \mid \beta_i \in [-1, 1] \right\}, \tag{22}$$

where $\boldsymbol{c} \in \mathbb{R}^n$ is the center and $\boldsymbol{g}_i \in \mathbb{R}^n$ are generators.

Therefore, by using (22), the uncertain input $\mathbf{P}$ in (1) can be expressed in a zonotope. For more accurate characterization of uncertainties, polynomial zonotypes and probabilistic zonotypes can be used [17].

B. Impact of Disturbances on the State Matrix

To calculate the reachable set, the state matrix needs to be updated at each time step, which is computationally expensive. Since only a few elements of the state matrix change as the disturbance happens, intuitively, this feature offers an option to update the state matrix in an efficient way, i.e., only re-calculating the affected elements. Therefore, we decompose the entire state matrix into two parts: submatrices correlated to disturbances and constant submatrices which do not change once the state matrix is built up. The following (23) is given as an example to show the impact of disturbances from DERs, loads, and the power exchange of each microgrid at the point of common coupling (PCC), respectively:

$$\mathbf{A}_P = \sum_{i=1}^{N_{NMG}} \mathbf{A}_i = \sum_{i=1}^{N_{NMG}} \times \left(\sum_{j=1}^{N_G} \mathbf{A}_i^{G_j} + \sum_{k=1}^{N_L} \mathbf{A}_i^{L_k} + \mathbf{A}_i^E + \mathbf{A}_i^{G,L,E} \right), \quad (23)$$

where N_{NMG} is the number of microgrids, N_G is the number of DERs in one microgrid, N_L is the number of loads in one microgrid, $\mathbf{A}_i$ is the increment of state matrix in the ith microgrid, $\mathbf{A}_i^{G_j}, \mathbf{A}_i^{L_k}, \mathbf{A}_i^E$ are the increments only correlated to DERs, loads, power exchange at PCC in the ith microgrid, and the cross items $\mathbf{A}_i^{G,L,E}$ represent their mutual effects on the matrix increment. Their expressions are given as follows:

$$\begin{aligned}
\mathbf{A}_i^{G_j} &= \mathbf{F}_\mathbf{x}^{G_j} - \mathbf{F}_\mathbf{y}^{G_j}\mathbf{G}_\mathbf{y}^{-1}\mathbf{G}_\mathbf{x}^{G_j} - \mathbf{F}_\mathbf{y}^{G_j}\mathbf{G}_\mathbf{y}^{-1}\mathbf{G}_\mathbf{x}^{C} \\
&\quad - \mathbf{F}_\mathbf{y}^{C}\mathbf{G}_\mathbf{y}^{-1}\mathbf{G}_\mathbf{x}^{G_j}, \\
\mathbf{A}_i^{L_k} &= \mathbf{F}_\mathbf{x}^{L_k} - \mathbf{F}_\mathbf{y}^{L_k}\mathbf{G}_\mathbf{y}^{-1}\mathbf{G}_\mathbf{x}^{L_k} - \mathbf{F}_\mathbf{y}^{L_k}\mathbf{G}_\mathbf{y}^{-1}\mathbf{G}_\mathbf{x}^{C} \\
&\quad - \mathbf{F}_\mathbf{y}^{C}\mathbf{G}_\mathbf{y}^{-1}\mathbf{G}_\mathbf{x}^{L_k}, \\
\mathbf{A}_i^{E} &= \mathbf{F}_\mathbf{x}^{E} - \mathbf{F}_\mathbf{y}^{E}\mathbf{G}_\mathbf{y}^{-1}\mathbf{G}_\mathbf{x}^{E} - \mathbf{F}_\mathbf{y}^{E}\mathbf{G}_\mathbf{y}^{-1}\mathbf{G}_\mathbf{x}^{C} - \mathbf{F}_\mathbf{y}^{C}\mathbf{G}_\mathbf{y}^{-1}\mathbf{G}_\mathbf{x}^{E}, \\
\mathbf{A}_i^{G_j,L_k} &= -\mathbf{F}_\mathbf{y}^{G_j}\mathbf{G}_\mathbf{y}^{-1}\mathbf{G}_\mathbf{x}^{L_k} - \mathbf{F}_\mathbf{y}^{L_k}\mathbf{G}_\mathbf{y}^{-1}\mathbf{G}_\mathbf{x}^{G_j}, \\
\mathbf{A}_i^{G_j,E} &= -\mathbf{F}_\mathbf{y}^{G_j}\mathbf{G}_\mathbf{y}^{-1}\mathbf{G}_\mathbf{x}^{E} - \mathbf{F}_\mathbf{y}^{E}\mathbf{G}_\mathbf{y}^{-1}\mathbf{G}_\mathbf{x}^{G_j}, \\
\mathbf{A}_i^{L_k,E} &= -\mathbf{F}_\mathbf{y}^{L_k}\mathbf{G}_\mathbf{y}^{-1}\mathbf{G}_\mathbf{x}^{E} - \mathbf{F}_\mathbf{y}^{E}\mathbf{G}_\mathbf{y}^{-1}\mathbf{G}_\mathbf{x}^{L_k}, \\
\mathbf{A}_i^{G,L,E} &= \mathbf{A}_i^{G_j,L_k} + \mathbf{A}_i^{G_j,E} + \mathbf{A}_i^{L_k,E},
\end{aligned}$$

where $\mathbf{F}_\mathbf{x}^{G_j}$, $\mathbf{F}_\mathbf{y}^{G_j}$, $\mathbf{G}_\mathbf{x}^{G_j}$ are matrices only related to the uncertainties from the jth DER unit in the ith microgrid, $\mathbf{F}_\mathbf{x}^{L_k}$, $\mathbf{F}_\mathbf{y}^{L_k}$, $\mathbf{G}_\mathbf{x}^{L_k}$ are matrices only related to the changes of the jth load in the ith microgrid, $\mathbf{F}_\mathbf{x}^{E}$, $\mathbf{F}_\mathbf{y}^{E}$, $\mathbf{G}_\mathbf{x}^{E}$ are matrices only related to the disturbances at PCC in the ith microgrid, $\mathbf{F}_\mathbf{x}^{C}$, $\mathbf{F}_\mathbf{y}^{C}$, $\mathbf{G}_\mathbf{x}^{C}$ are constant matrices uncorrelated with any disturbances.

The above decomposition has the following advantages:

1) It becomes easy and efficient to calculate the increment $\mathbf{A}_P$ when disturbances occur, because only specific sub-matrices need to be updated.
2) It provides an efficient tool to analyze the impacts of disturbances. For instance, it can be clearly observed from (23) that the increment of the state matrix can be expressed in the form of a combination of disturbances, which makes it easier to analyze the impact of a specific disturbance.
3) In particular, it can seamlessly combine with zonotope modeling. After calculating zonotopes of sub-matrices, we can efficiently update the zonotope of $\mathbf{A}_P$ which can be subsequently applied in the quasi-diagonalized Geršgorin Theorem to get Geršgorin disks.

V. Stability Margin Estimation Via FAR Integrated With Enhanced Geršgorin Theorem

When reachable sets are obtained via FAR, it is still necessary to know how far a networked microgrids system is from its stability margin, especially when the system is operating in the islanding mode. First, it is important to ensure a sufficient stability margin exists in the system at all times. Second, predictive control or dispatch can be performed in advance if the system is found approaching its stability margin. Third, only when networked microgrids have sufficient stability margins, they can serve as resiliency sources to actively and coordinately provide ancillary services that stabilize, restore, or black start the main grid.

FAR integrated with the quasi-diagonalized Geršgorin theory offers an option to effectively calculate and analyze stability margins for a networked microgrids system. The analysis procedure is presented as follows: first, FAR is used to calculate the reachable set $\mathcal{R}^e(t_k)$ of a system under disturbances. The edge of the reachable set is then extracted for quasi-diagonalized Geršgorin calculation by using (15) and (16). Finally, the corresponding Geršgorin disk is sequentially evaluated to assess the stability condition under disturbances. The procedures of stability margin calculation and analysis via FAR integrated with quasi-diagonalized Geršgorin Theorem are illustrated in Fig. 1.

In Fig. 1, a networked microgrids system including feeder sections, transformers, and loads is initially modeled, and the dynamics of power-electronic-interfaces and DERs are then formulated via a set of differential equations. A typical power-electronic-interfaced microgrid is shown in the Appendix. After that, power flow is formulated and calculated, where an extended admittance matrix-based method is adopted to simplify the calculation process. The extended admittance matrix method is introduced as follows:

A. Extended Admittance Matrix-Based Power Flow

Assume the admittance between node *i* and node *j* is $Y_{ij} = |Y_{ij}|\cos(\alpha_{ij}) + j|Y_{ij}|\sin(\alpha_{ij})$. The power injection from node *i* to node *j* can then be expressed as:

$$\begin{aligned}
P_{ij} &= V_i V_j |Y_{ij}| \cos(\theta_i - \theta_j - \alpha_{ij}), \\
Q_{ij} &= V_i V_j |Y_{ij}| \sin(\theta_i - \theta_j - \alpha_{ij}),
\end{aligned}$$

where V_i, V_j are the voltage amplitudes at the node *i* and node *j*, θ_i, θ_j are the voltage angles at the node *i* and node *j*, $|Y_{ij}|$ is the absolute value of the branch admittance between the node *i* and node *j*, and α_{ij} is the corresponding angle of the branch admittance.

Then the power flow equation can be expressed as follows:

$$\begin{aligned}
&\begin{bmatrix} |Y_{ij}|\cos(\theta_i - \theta_j - \alpha_{ij}) \\ |Y_{ij}|\sin(\theta_i - \theta_j - \alpha_{ij}) \end{bmatrix} \cdot \begin{bmatrix} V_{ij} \end{bmatrix} \circ \begin{bmatrix} V_{ij} \\ V_{ij} \end{bmatrix} + \begin{bmatrix} P_{ij}^G \\ Q_{ij}^G \end{bmatrix} \\
&\quad - \begin{bmatrix} P_{ij}^L \\ Q_{ij}^L \end{bmatrix} \\
&= \overline{\mathbf{Y}} \cdot \mathbf{V} \circ \overline{\mathbf{V}} + \overline{\mathbf{S}^G} - \overline{\mathbf{S}^L} = \mathbf{0}, \quad (24)
\end{aligned}$$

where $\circ$ is the Hadamard product, P_{ij}^G, Q_{ij}^G are the active and reactive power injection from DERs to the node *j*, and P_{ij}^L, Q_{ij}^L are the active and reactive power load at the node *j*.

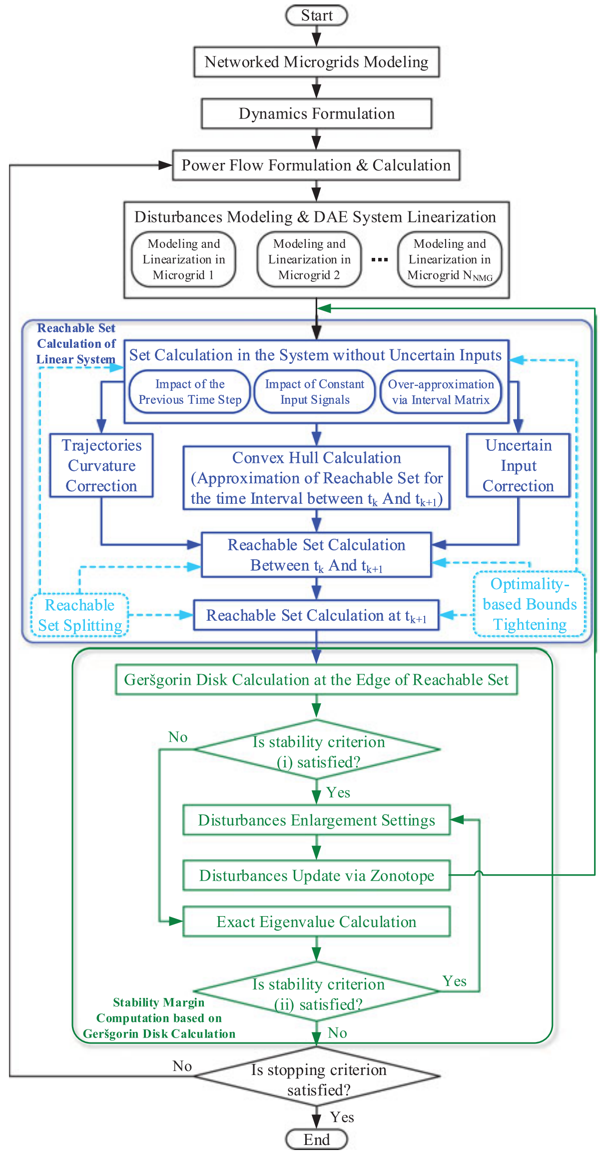

Fig. 1. Flowchart of reachable set calculation and stability margin evaluation.

The advantages of the extended admittance matrix-based power flow formulation include:

1) The admittance is formulated in modules, which enables 'plug and play' and easy removal of components such as DERs or even microgrids.
2) It offers an option to directly analyze the impact of uncertainties on power flow results. For instance, when P_{ij}^G, Q_{ij}^G are expressed in zonotopes, (24) will give power flow zonotopes that enclose the effects of disturbances.

B. Reachable Set and Stability Margin Calculation

After the power flow is calculated, system linearization can be conducted via (19), based on which reachable set can be calculated via (2) and (3). When the reachable set at t_{k+1} is obtained, the quasi-diagonalized Geršgorin Theorem is used to estimate the eigenvalue distribution at the edge of the reachable set. The analysis process is given as follows:

1) If the following stability criterion (i) is satisfied, it means the study system is stable; otherwise, the system may not be stable, and a QR analysis will be performed to calculate the exact eigenvalues to validate the stability.

$$s_{kk}^{\max} + r_k^{\max}(\mathbf{S}_P) \le \alpha_0 \quad (\text{Stability criterion}(i)), \tag{25}$$

where $s_{kk}^{\max}$ is the center of Geršgorin disk which is located in the rightest hand, $r_k^{\max}(\mathbf{S}_P)$ is the corresponding radius, and α_0 is the given threshold.

2) If the study system is stable, disturbances will be enlarged in order to get the stability margin. After setting new disturbances, the reachable set will be calculated correspondingly and Geršgorin estimation will be conducted as well to evaluate the stability again.
3) If the stability criterion (i) is not satisfied, after calculating the exact eigenvalues, stability criterion (ii) will be used to evaluate the stability.

$$\alpha_{\max} \le \alpha_0 \quad (\text{Stability criterion}(ii)), \tag{26}$$

where $\alpha_{\max}$ is the real part of the maximum eigenvalue.

4) The evaluation process will be terminated when the simulation time ends or the system is always unstable after a given simulation steps. If one of these criteria is satisfied, then stop; otherwise continue power flow calculation and reachable set computation.

Therefore, the presented quasi-diagonalized Gergorin theory enables efficient eigenvalues estimation of dynamic systems under disturbances. Specifically, if we adopt the exact calculation method, each time a disturbance happens, state matrix update, Householder transformation, Hessenberg matrix formation, QR decomposition, etc. [24], need to be conducted to calculate the exact eigenvalues. In contrast, by using the proposed quasi-diagonalized Gergorin theory, only the increment of the state matrix shown in (23) needs to be calculated. Thus, eigenvalues can be efficiently estimated via (15)–(17), which makes the above complex procedures of exact eigenvalue calculation unnecessary. Besides, oftentimes we do not need to know the exact eigenvalues. For instance, if the largest eigenvalue approximated through quasi-diagonalized Gergorin theory is located on the left half plane and far away from y-axis, it means the system is absolutely stable, because quasi-diagonalized Gergorin results must cover all possible eigenvalues; thus, it indicates there is no need to obtain the exact eigenvalues to figure out the stability of a dynamic system.

Note that the system's stability is assessed via eigenvalue locations at reachable points per request, which may result in a conservative evaluation. The reasons include: (i) system linearization may introduce errors even the eigenvalues are exactly calculated through QR algorithm, and (ii) each reachable point is treated as an equilibrium point, which may lead to a conservative result. Thus, this is a limitation to be overcome in the future. One possible solution is to combine the presented FAR with the time domain stability approaches introduced in [25].

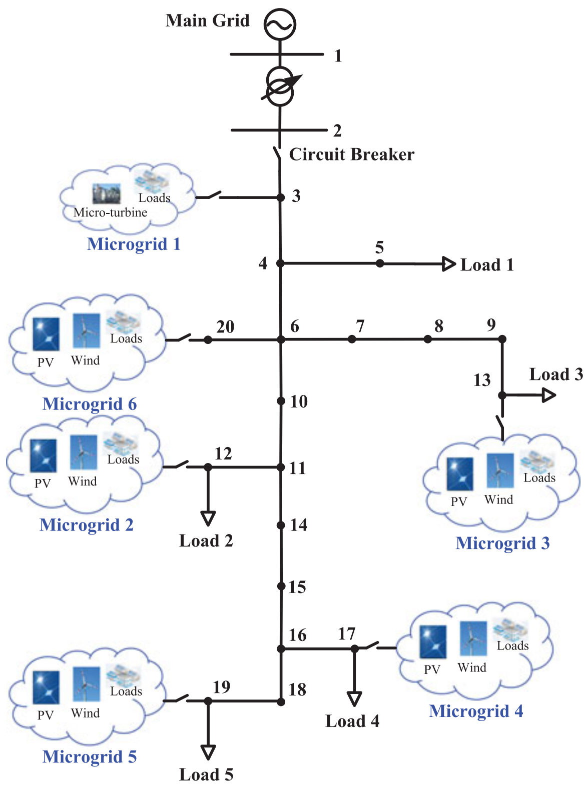

Fig. 2. A typical networked microgrids system.

VI. Test and Validation of FAR

A typical networked microgrids system shown in Fig. 2 is used to test and validate the presented FAR approach integrated with quasi-diagonalized Geršgorin Theorem. The networked microgrids system is assumed to operate in islanded mode to better illustrate the impact of disturbances. The test system includes six microgrids. Microgrid 1 is powered by a small conventional generator represented by a classical synchronous generator [17], controlling the voltage and frequency in the system. The other microgrids are power-electronic-dominant systems equipped with inverters and their controller using power control strategy as shown in the Appendix. The system in Fig. 2 has a 36×18 extended admittance matrix $\overline{\mathbf{Y}}$ when it is operated in the islanded mode. The dimensions of the node voltage vector $\mathbf{V}$, the extended node voltage vector $\overline{\mathbf{V}}$, and node power vector $\overline{\mathbf{S}^G}, \overline{\mathbf{S}^L}$ are 18×1, 36×1, 36×1 and 36×1, respectively. Parameters for microgrid controllers are summarized in the Appendix while those of the backbone system can be found in [26]. The FAR algorithms are developed on the basis of multiple functions in the CORA toolbox [27]. The simulation step size is set to 0.010 s.

A. Reachable Set Calculation Via FAR

1) Reachable Set Calculation: In this test, the active power output in Microgrid 6 fluctuates around its baseline power by $\pm 5\%, \pm 10\%, \pm 15\%$ and $\pm 20\%$. Under these uncertainties, the reachable sets of X_{pi}, X_{qi} in Microgrids 6, 2 and 5 are given in

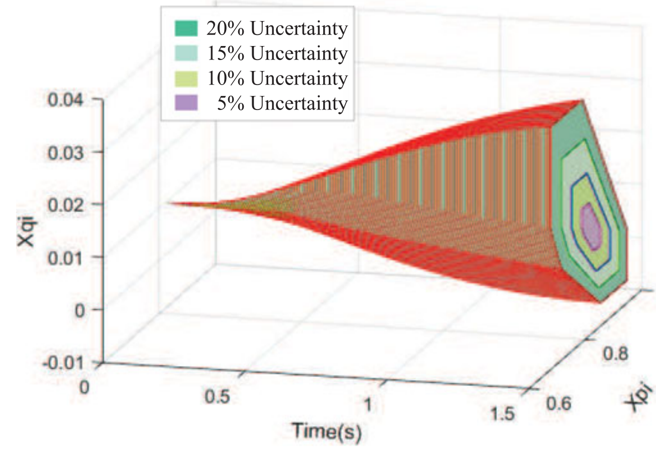

Fig. 3. 3-D reachable set of X_{pi}, X_{qi} in Microgrid 6.

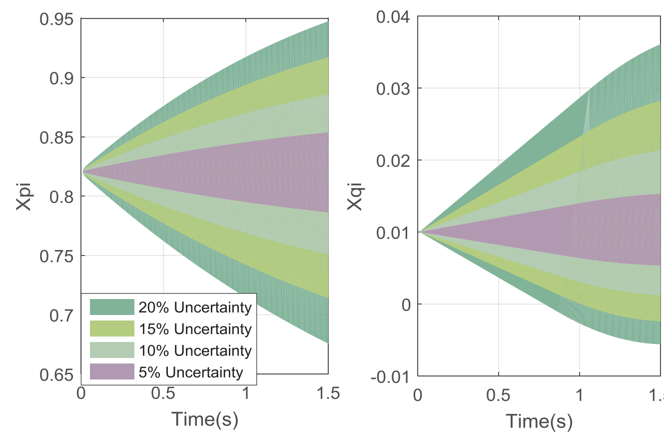

Fig. 4. Reachable set of X_{pi}, X_{qi} in Microgrid 6 projected to the time line.

Figs. 3, 5 and 7, and Figs. 4, 6 and 8 show the cross sectional views of reachable set along the time line. Here X_{pi} is the state variable in the upper proportional-integral block, whereas X_{qi} is the state variable in the lower proportional-integral block (see the Appendix), which are the key variables to control inverter. It can be seen that:

1) The possible operation range of a networked microgrids system under disturbances can be directly obtained via reachable set calculation. The simulation time is equivalent to just a few runs of deterministic time domain simulations, meaning FAR is efficient.
2) The sizes of zonotopes along reachtubes increase as the uncertainty level increases. Its correctness and overapproximation are further demonstrated by the comparison with time domain simulations in the next section.
3) The results in Figs. 3 and 4 show that the reachable sets pertaining to Microgrid 6 are converging rather than consistently increasing along the timeline. The reason is that Microgrids 6 is electrically close to Microgrid 1 which consists of a synchronous generator. Thus, the impact of uncertainties are alleviated by the inertia in Microgrid 1.

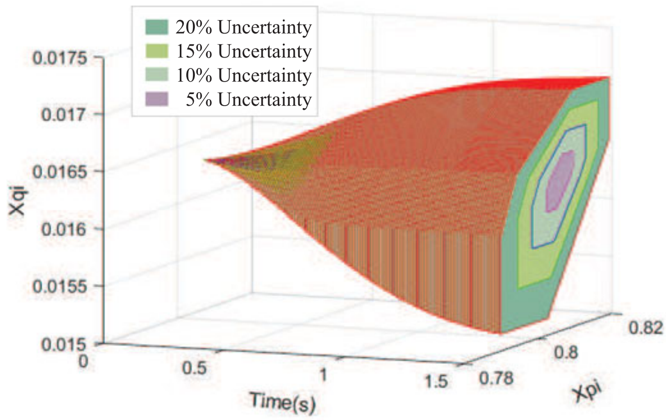

Fig. 5. 3-D reachable set of X_{pi}, X_{qi} in Microgrid 2.

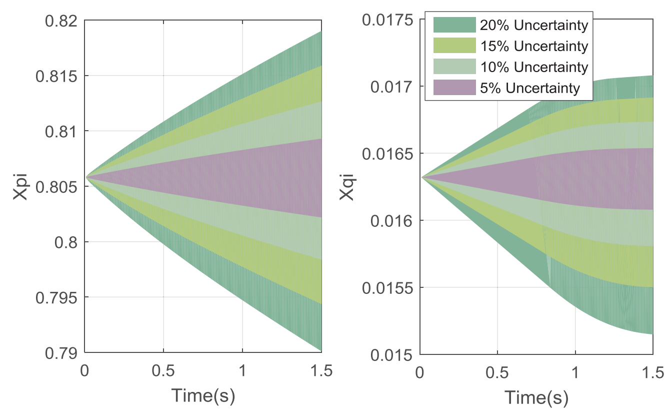

Fig. 6. Reachable set of X_{pi}, X_{qi} in Microgrid 2 projected to the time line.

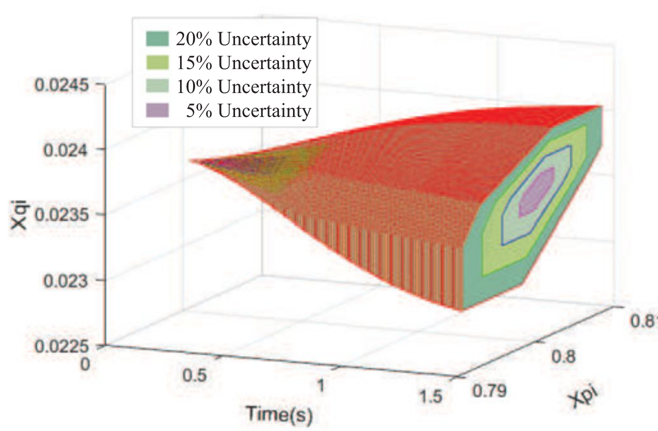

Fig. 7. 3-D reachable set of X_{pi}, X_{qi} in Microgrid 5.

4) The reactive power output of microgrids is impacted considerably by the fluctuations in active power, even when the changes in active power are very small. This is largely attributed to the presence of resistances in the backbone feeders [28].
5) The comparison between Figs. 5 and 7 shows that the impact of disturbances in Microgrid 6 have less impact on the dynamics of Microgrid 5 than those of Microgrid 2, because Microgrid 5 is electrically the farthest one from Microgrid 6. For instance, according to Figs. 6 and 8, at 1.5 s, the deviations of X_{pi} and X_{qi} in Microgrid 2 under 20% disturbance are $[-1.95\%, 1.64\%]$ and $[-7.18\%, 4.65\%]$, whereas those deviations in Microgrid 5 are $[-1.20\%, 1.01\%]$ and $[-2.78\%, 1.86\%]$ which are smaller than those in the Microgrid 2.

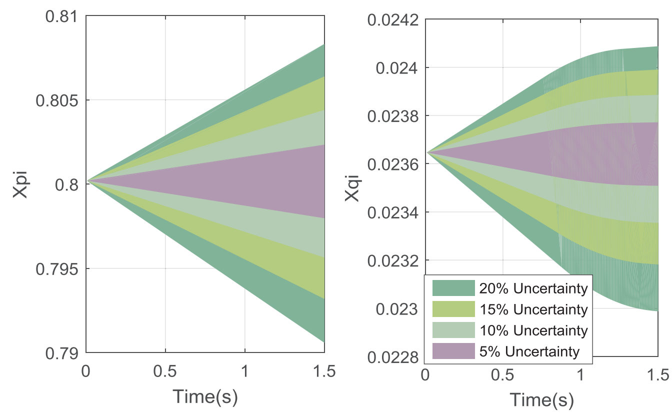

Fig. 8. Reachable set of X_{pi}, X_{qi} in Microgrid 5 projected to the time line.

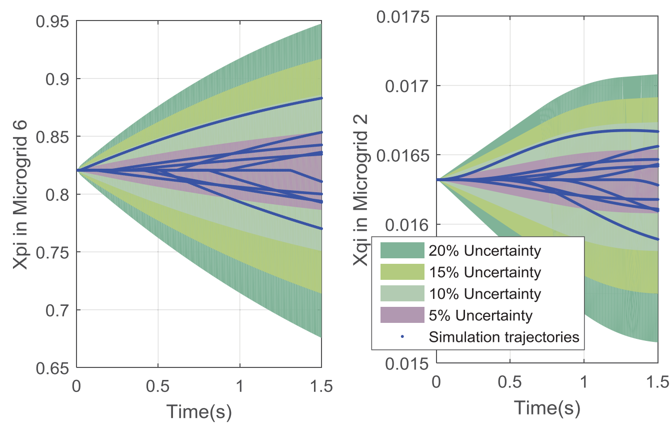

Fig. 9. Time domain simulation verification.

2) Reachable Set Verification Via Time Domain Simulations: Time domain simulations are used to verify the effectiveness of FAR. For clear illustration, ten simulation trajectories are selected to compare against the FAR results. Fig. 9 shows the simulation results of X_{pi} and X_{qi}. It can be observed that:

1) The time domain trajectories are fully enclosed by reachable sets, which validates the over-approximation capability of FAR.
2) In this test case, the conservativeness of reachable sets is acceptable and actually desirable; however, when the system scale increases drastically, techniques to reduce conservativeness such as set splitting or optimality-based bounds tightening may become necessary.

3) Efficiency of FAR: The computation times for the ten time domain simulations in *2)* versus reachable set calculation are

TABLE I
CALCULATION TIMES FOR 1.5 S DYNAMICS ON A 3.4 GHz PC

Cases \ Uncertainties	20%	15%	10%	5%
FAR Time (s)	8.3311	8.1483	7.6262	7.6025
Time Domain Simulation Time (s)	6.4853	6.1576	6.4217	6.3235

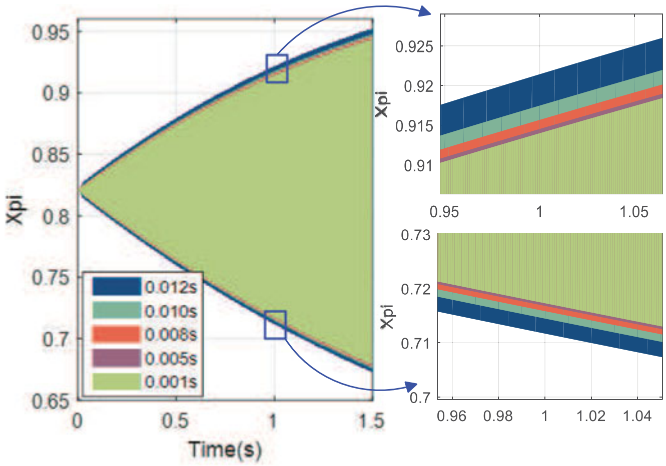

Fig. 10. FAR results comparison between different step sizes.

TABLE II
CALCULATION TIME AND RELATIVE ERRORS USING DIFFERENT SIMULATION STEP SIZES

Step Size (s)	Simulation Time (s)	Relative Errors (%)
0.001	75.3687	0.0000
0.005	16.8564	0.0584
0.008	10.7814	0.2238
0.010	8.3311	0.3107
0.012	6.5290	0.7810

given in Table I, which validate FAR is an efficient approach in analyzing system dynamics under uncertainties.

4) Simulation Step Size Discussion: Since the networked microgrids is a nonlinear system, step size will affect the FAR accuracy. Fig. 10 shows the comparison of X_{pi} in Microgrid 6 between different step sizes when $\pm 20\%$ active power uncertainty happens in Microgrid 6. Fig. 10 offers the following findings:

1) When the time step is set as 0.001 s, a relatively accurate result can be obtained; but it takes much longer time to finish the FAR calculation.
2) As the step size increases, the simulation time decreases, and so does the calculation accuracy. Table II summarizes the calculation time using different step sizes.
3) When the step size is set as 0.015 s, the simulation process suspends after 15 steps, because the matrix $\mathbf{G_y}$ is close to singular or badly scaled; and thus, results may be inaccurate. Especially, when the time step reaches 0.05 s, the simulation process stops after only three steps.
4) Assume the result of 0.001 s time step is accurate, the relative errors of the other time steps at 1.0 s are given in Table II.

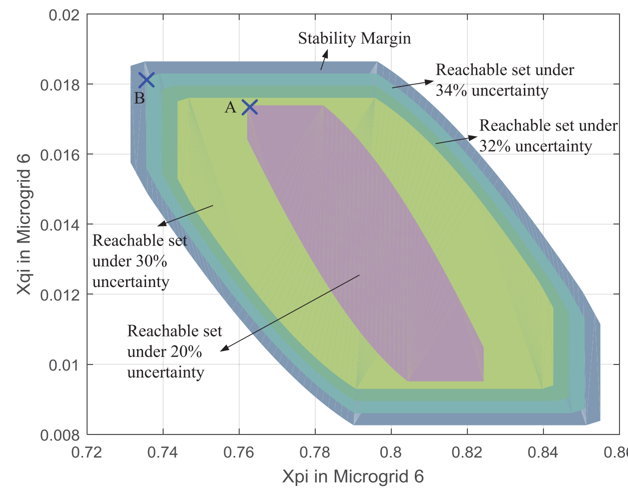

Fig. 11. Stability margin of Microgrid 6 at 0.5 s.

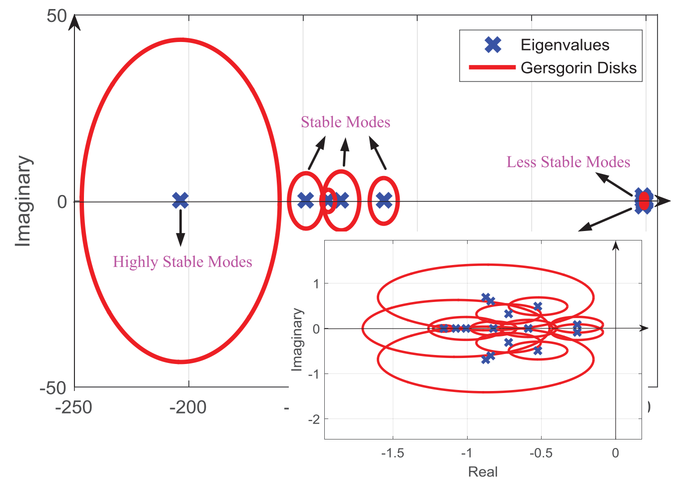

Fig. 12. Geršgorin disks and eigenvalues of point A.

5) Therefore, more accurate results can be obtained by using a very small simulation step, e.g., 0.001 s; however, it is very time consuming. On the other hand, an excessively large simulation step may accelerate FAR calculation at the expense of inaccurate results or even halt. Thus, taking into account the simulation time and calculation accuracy, the step size of 0.010 s is selected for both efficient and accurate stability evaluation.

B. Stability Margin Calculation Via FAR and Quasi-Diagonalized Geršgorin Theorem

1) Stability Margin Calculation: This case demonstrates the usefulness of quasi-diagonalized Geršgorin Theorem in evaluating the stability margins at different time points. Fig. 11 shows the stability margin of Microgrid 6 at 0.5 s; Figs. 12 and 13 illustrate the corresponding Geršgorin disks at vertices A and B in Fig. 11 with exact eigenvalues given as well. It can be seen that:

1) The stability margin can be efficiently obtained, which verifies the feasibility of FAR and quasi-diagonalized Geršgorin Theorem.

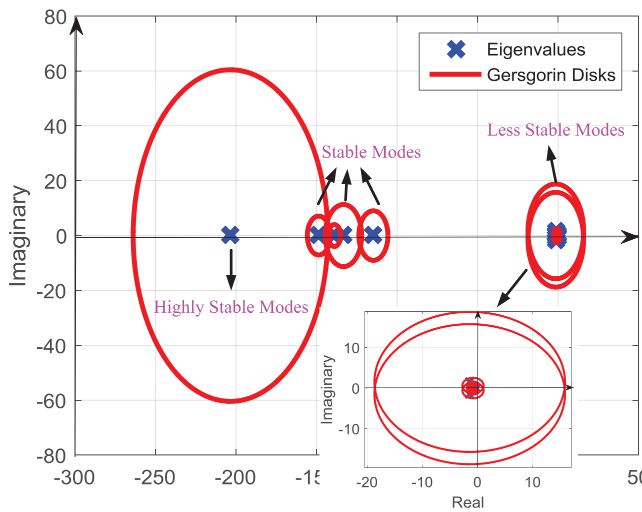

Fig. 13. Geršgorin disks and eigenvalues of point B.

2) Quasi-diagonalized Geršgorin Theorem can effectively assess the stability when the system operation point is far away from its stability margin, e.g., the point A in Fig. 11. It makes exact eigenvalue calculation unnecessary.
3) When the system is approaching its stability margin, results from quasi-diagonalized Geršgorin can be conservative (e.g., the point B's stability results shown in Fig. 13), and thus, exact eigenvalue inspection is needed.
4) Eigenvalue results show that there exist three groups of dynamic modes, i.e., 'less stable modes,' 'stable modes,' and 'highly stable modes' as show in Figs. 12 and 13. Since eigenvalues of less stable modes dominate the system's dynamics, attention should be paid to the Geršgorin disks calculation in this area, as the zoomed-in plots shown in Figs. 12 and 13.

2) Efficiency of Quasi-Diagonalized Geršgorin Theorem: According to Fig. 1, quasi-diagonalized Geršgorin Theorem based eigenvalue estimation will be performed until stability criterion *(i)* is not met. In the worst case, exact eigenvalue is calculated at each time step, which takes 29.8990 s. However, the quasi-diagonalized Geršgorin Theorem based evaluation only takes 17.1653 s, which is only 57.41% of the time used in the exact eigenvalue calculation case. The computational time comparison validates the quasi-diagonalized Gergorin Theorem is an efficient approach in evaluating system stability under uncertainties.

3) Applications of FAR in Networked Microgrids Operation: One of the operators concerns in operating a networked microgrids system is how to reliably assess its stability for improving the situational awareness and controllability so that it can be used as dependable resiliency resource. The FAR results on stability margin enable operators to take the following actions:
1) Forecast and monitor networked microgrids performance, so that the operators can have a better understanding about the dynamics of a networked microgrids system under high-penetration of renewable generation.
2) Perform predictive control or dispatch in advance if the system is found approaching its stability margin, e.g., point B in Fig. 11, such that the stability and resiliency of the networked microgrids system can be significantly improved.
3) Pinpoint the critical components or controls of a networked microgrids system (e.g., those with high trajectory sensitivities), which inform the operator the most cost-effective measures to enlarge stability region of microgrids.

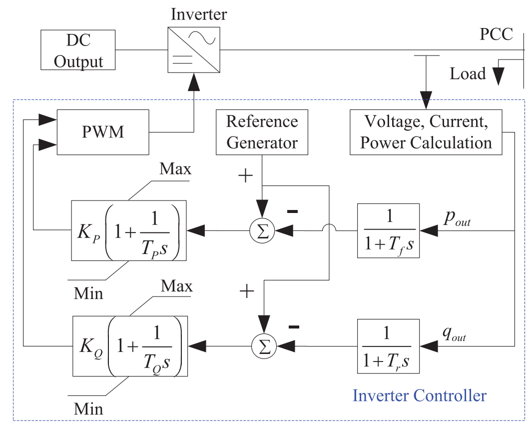

Fig. 14. Power-electronic-dominant microgrid equivalent model.

TABLE III
PARAMETERS FOR INVERTER CONTROLLERS IN MICROGRIDS

Microgrids	Parameters T_f	T_r	K_P	T_P	K_Q	T_Q
2	0.01	0.01	0.45	0.02	0.45	0.02
3	0.01	0.01	0.80	0.01	0.80	0.01
4	0.01	0.01	0.50	0.02	0.50	0.02
5	0.01	0.01	0.30	0.02	0.30	0.02
6	0.01	0.01	0.40	0.02	0.40	0.02

VII. CONCLUSION

The paper contributes a new formal stability assessment theory, FAR, for deeper understanding of networked microgrid resilience under high penetration level of renewable generation. With efficient system linearization, zonotope modeling, and stability region estimation, FAR is able to increase situational awareness and thus unlock the potential of networked microgrids as primary resilience resources. Test results demonstrate the efficiency and effectiveness of FAR.

In the future, the formal analysis approach can be further evaluated on a real time simulation testbed and integrated in the advanced distribution management systems (ADMS) to provide situational awareness and forecast operation margin and stability margin of networked microgrids.

APPENDIX
POWER-ELECTRONIC-DOMINANT MICROGRID EQUIVALENT CIRCUIT

The power-electronic-dominant microgrids equivalent model is shown in Fig. 14 with controller parameters in each microgrid given in Table III.

ACKNOWLEDGMENT

The authors would like to thank Matthias Althoff from Technische Universität München, Germany, for the helpful discussion. The authors also would like to thank the anonymous reviewers for the valuable comments.

REFERENCES

[1] R. H. Lasseter and P. Paigi, "Microgrid: A conceptual solution," in *Proc. 2004 IEEE 35th Annu. Power Electron. Spec. Conf.*, vol. 6, 2004, pp. 4285–4290.

[2] Z. Bie, P. Zhang, G. Li, B. Hua, M. Meehan, and X. Wang, "Reliability evaluation of active distribution systems including microgrids," *IEEE Trans. Power Syst.*, vol. 27, no. 4, pp. 2342–2350, Nov. 2012.

[3] F. Shahnia, S. Bourbour, and A. Ghosh, "Coupling neighboring microgrids for overload management based on dynamic multicriteria decision-making," *IEEE Trans. Smart Grid*, vol. 8, no. 2, pp. 969–983, Mar. 2012.

[4] Z. Wang, B. Chen, J. Wang, M. M. Begovic, and C. Chen, "Coordinated energy management of networked microgrids in distribution systems," *IEEE Trans. Smart Grid*, vol. 6, no. 1, pp. 45–53, Jan. 2015.

[5] C. Wang, Y. Li, K. Peng, B. Hong, Z. Wu, and C. Sun, "Coordinated optimal design of inverter controllers in a micro-grid with multiple distributed generation units," *IEEE Trans. Power Syst.*, vol. 28, no. 3, pp. 2679–2687, Aug. 2013.

[6] N. Duan and K. Sun, "Power system simulation using the multistage adomian decomposition method," *IEEE Trans. Power Syst.*, vol. 32, no. 1, pp. 430–441, Jan. 2017.

[7] H.-D. Chang, C.-C. Chu, and G. Cauley, "Direct stability analysis of electric power systems using energy functions: theory, applications, and perspective," *Proc. IEEE*, vol. 83, no. 11, pp. 1497–1529, Nov. 1995.

[8] C. Canizares *et al.*, "Benchmark models for the analysis and control of small-signal oscillatory dynamics in power systems," *IEEE Trans. Power Syst.*, vol. 32, no. 1, pp. 715–722, Jan. 2017.

[9] T.-E. Huang, Q. Guo, and H. Sun, "A distributed computing platform supporting power system security knowledge discovery based on online simulation," *IEEE Trans. Smart Grid*, vol. 8, no. 3, pp. 1513–1524, May 2017.

[10] H.-D. Chiang, F. Wu, and P. Varaiya, "Foundations of direct methods for power system transient stability analysis," *IEEE Trans. Circuits Syst.*, vol. 34, no. 2, pp. 160–173, Feb. 1987.

[11] W. Lohmiller and J.-J. E. Slotine, "On contraction analysis for non-linear systems," *Automatica*, vol. 34, no. 6, pp. 683–696, 1998.

[12] E. M. Aylward, P. A. Parrilo, and J.-J. E. Slotine, "Stability and robustness analysis of nonlinear systems via contraction metrics and sos programming," *Automatica*, vol. 44, no. 8, pp. 2163–2170, 2008.

[13] A. P. Dani, S.-J. Chung, and S. Hutchinson, "Observer design for stochastic nonlinear systems via contraction-based incremental stability," *IEEE Trans. Automat. Control*, vol. 60, no. 3, pp. 700–714, Mar. 2015.

[14] C. Juarez and A. Stankovic, "Contraction analysis of power system dynamics using time-varying OMIB equivalents," in *Proc. 39th North Amer. Power Symp.*, 2007, pp. 385–391.

[15] A. Papachristodoulou and S. Prajna, "Analysis of non-polynomial systems using the sum of squares decomposition," in *Positive Polynomials in Control*. New York, NY, USA: Springer, 2005, pp. 23–43.

[16] P. A. Parrilo, "Semidefinite programming relaxations for semialgebraic problems," *Math. Program.*, vol. 96, no. 2, pp. 293–320, 2003.

[17] M. Althoff, "Formal and compositional analysis of power systems using reachable sets," *IEEE Trans. Power Syst.*, vol. 29, no. 5, pp. 2270–2280, Sep. 2014.

[18] M. Althoff and B. H. Krogh, "Zonotope bundles for the efficient computation of reachable sets," in *Proc. 2011 50th IEEE Conf. Decis. Control Eur. Control Conf.*, 2011, pp. 6814–6821.

[19] Y. Li, P. Zhang, L. Ren, and T. Orekan, "A Geršgorin theory for robust microgrid stability analysis," in *Proc. PES Gen. Meeting*, 2016, pp. 1–5.

[20] M. Althoff, O. Stursberg, and M. Buss, "Reachability analysis of nonlinear systems with uncertain parameters using conservative linearization," in *Proc. 47th IEEE Conf. Decis. Control*, 2008, pp. 4042–4048.

[21] T. Ding *et al.*, "Interval power flow analysis using linear relaxation and optimality-based bounds tightening (OBBT) methods," *IEEE Trans. Power Syst.*, vol. 30, no. 1, pp. 177–188, Jan. 2015.

[22] L. Cvetkovic, V. Kostic, and R. S. Varga, "A new Geršgorin-type eigenvalue inclusion set," *Electron. Trans. Numer. Anal.*, vol. 18, pp. 73–80, 2004.

[23] M. M. Moldovan and M. S. Gowda, "Strict diagonal dominance and a Geršgorin type theorem in Euclidean Jordan algebras," *Linear Algebra Appl.*, vol. 431, no. 1, pp. 148–161, 2009.

[24] J. H. Wilkinson, *The Algebraic Eigenvalue Problem*. Oxford, U.K.: Clarendon, 1965.

[25] K. Clements and J. Wall, "Time domain stability margin assessment of the NASA space launch system GN&C design for exploration mission one," NASA, Washington, DC, USA, Rep. no. M17-5829, 2017.

[26] S. Papathanassiou *et al.*, "A benchmark low voltage microgrid network," in *Proc. CIGRE Symp., Power Syst. Dispersed Gener.*, 2005, pp. 1–8.

[27] M. Althoff, *CORA 2016 Manual*. Technische Universitat Munchen, Garching, Germany, 2016.

[28] N. Pogaku, M. Prodanovic, and T. C. Green, "Modeling, analysis and testing of autonomous operation of an inverter-based microgrid," *IEEE Trans. Power Electron.*, vol. 22, no. 2, pp. 613–625, Mar. 2007.

Yan Li (S'13) received the B.Sc. and M.Sc. degrees in electrical engineering from Tianjin University, Tianjin, China, in 2008 and 2010, respectively. She is currently working toward the Ph.D. degree in electrical engineering at the University of Connecticut, Storrs, CT, USA. Her research interests include microgrids and networked microgrids, formal analysis, power system stability and control, software-defined networking, and cyber-physical security.

Peng Zhang (M'07–SM'10) received the Ph.D. degree in electrical engineering from the University of British Columbia, Vancouver, BC, Canada, in 2009. He is the Castleman Professor in Engineering Innovation and an Associate Professor of Electrical Engineering with the University of Connecticut, Storrs, CT, USA. He was a System Planning Engineer with BC Hydro and Power Authority, Vancouver. His research interests include microgrids, power system stability and control, cyber security, and smart ocean systems. Dr. Zhang is a Registered Professional Engineer in BC, Canada, and an individual member of CIGRÉ.

Peter B. Luh (S'77–M'80–SM'91–F'95–LF'16) received the B.S. degree from the National Taiwan University, Taipei, Taiwan, the M.S. degree from the Massachusetts Institute of Technology, Cambridge, MA, USA, and the Ph.D. degree from Harvard University, Cambridge, MA, USA. He has been with the Department of Electrical and Computer Engineering, University of Connecticut, Storrs, CT, USA, since 1980, and is the SNET Professor of Communications and Information Technologies. He is also a Member of the Chair Professors Group with the Department of Automation, Tsinghua University, Beijing, China. His research interests include smart grid, intelligent manufacturing systems, and energy smart buildings. He is the Chair of the IEEE TAB Periodicals Committee, and was the founding Editor-in-Chief for the IEEE TRANSACTIONS ON AUTOMATION SCIENCE AND ENGINEERING, and an Editor-in-Chief for the IEEE TRANSACTIONS ON ROBOTICS AND AUTOMATION. He is a recipient of the IEEE Robotics and Automation Society 2013 Pioneer Award for his contributions to the development of near-optimal and efficient planning, scheduling, and coordination methodologies for manufacturing and power systems; and the 2017 George Saridis Leadership Award for his exceptional vision and leadership in strengthening and advancing automation.